

Supplemental materials for:

Unraveling patterns of disrupted gene expression across a complex tissue

Kelsie E. Hunnicutt, Jeffrey M. Good, and Erica L. Larson

Supplemental Figures:

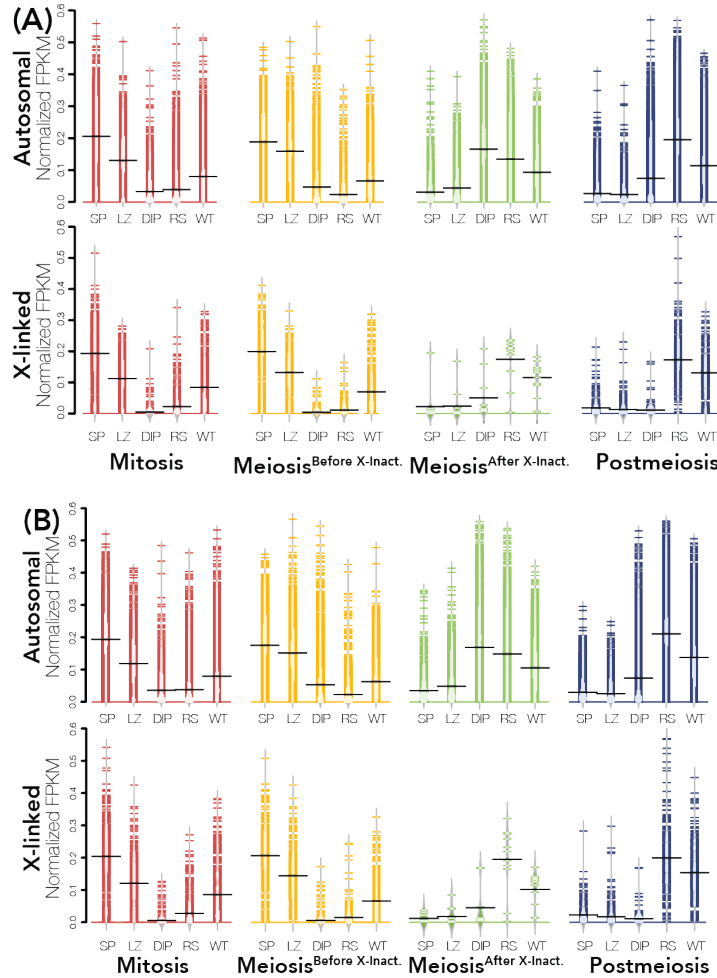


Figure S1. Expression of induced genes in *mus* and *dom* samples. For each sorted cell population, we defined a set of induced genes in parental samples that had a median expression two times greater than the median expression of those genes across the remaining cell types. Expression of induced genes in *mus* (A) and *dom* (B) individuals is plotted across all sample types (SP = Mitosis, LZ = Meiosis^{Before X-Inact.}, DIP = Meiosis^{After X-Inact.}, RS = Postmeiosis, and WT = Whole Testes) with cell type of induced genes indicated by color (red = Mitosis, yellow = Meiosis^{Before X-Inact.}, green = Meiosis^{After X-Inact.}, and blue = Postmeiosis). FPKM is normalized so that the sum of squares equals 1 using the R package vegan (Oksanen et al. 2007).

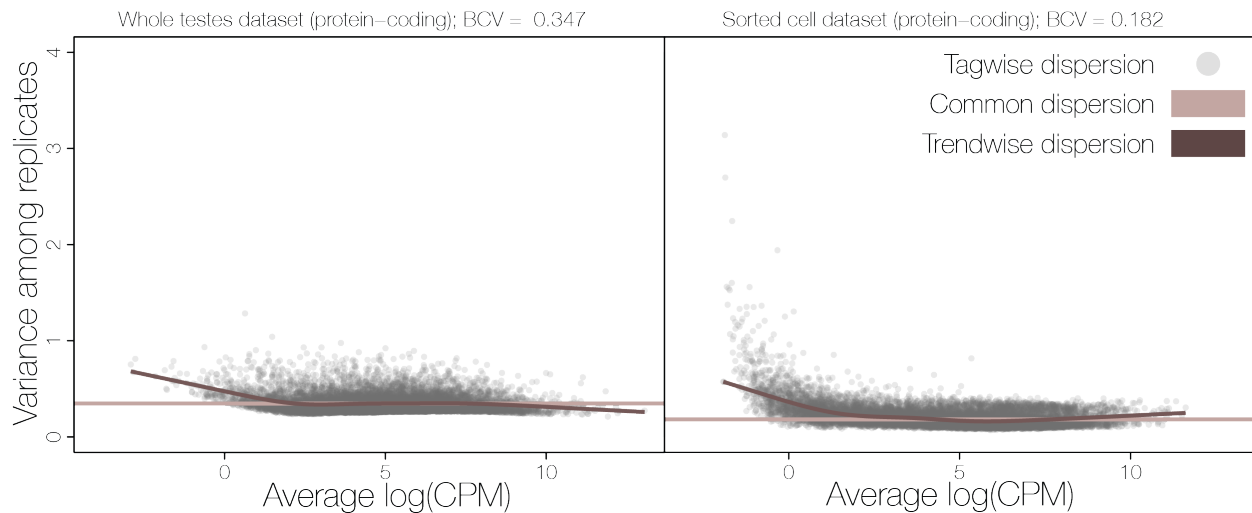


Fig S2. Dispersion estimates and biological coefficients of variation (BCV) across protein-coding genes for the whole testes and sorted cell datasets. All dispersion estimates were calculated in R with the edgeR package (McCarthy et al. 2012). Common dispersion for each dataset is calculated using a common estimate across all genes (taupe line). The trendwise dispersion calculation fits an estimate of dispersion based on the mean-variance trend across the entire dataset so that genes with similar abundances have similar variance estimates (brown line). Tagwise dispersion estimates dispersion on a per gene basis (gray dots). The BCV is the square root of the common dispersion.

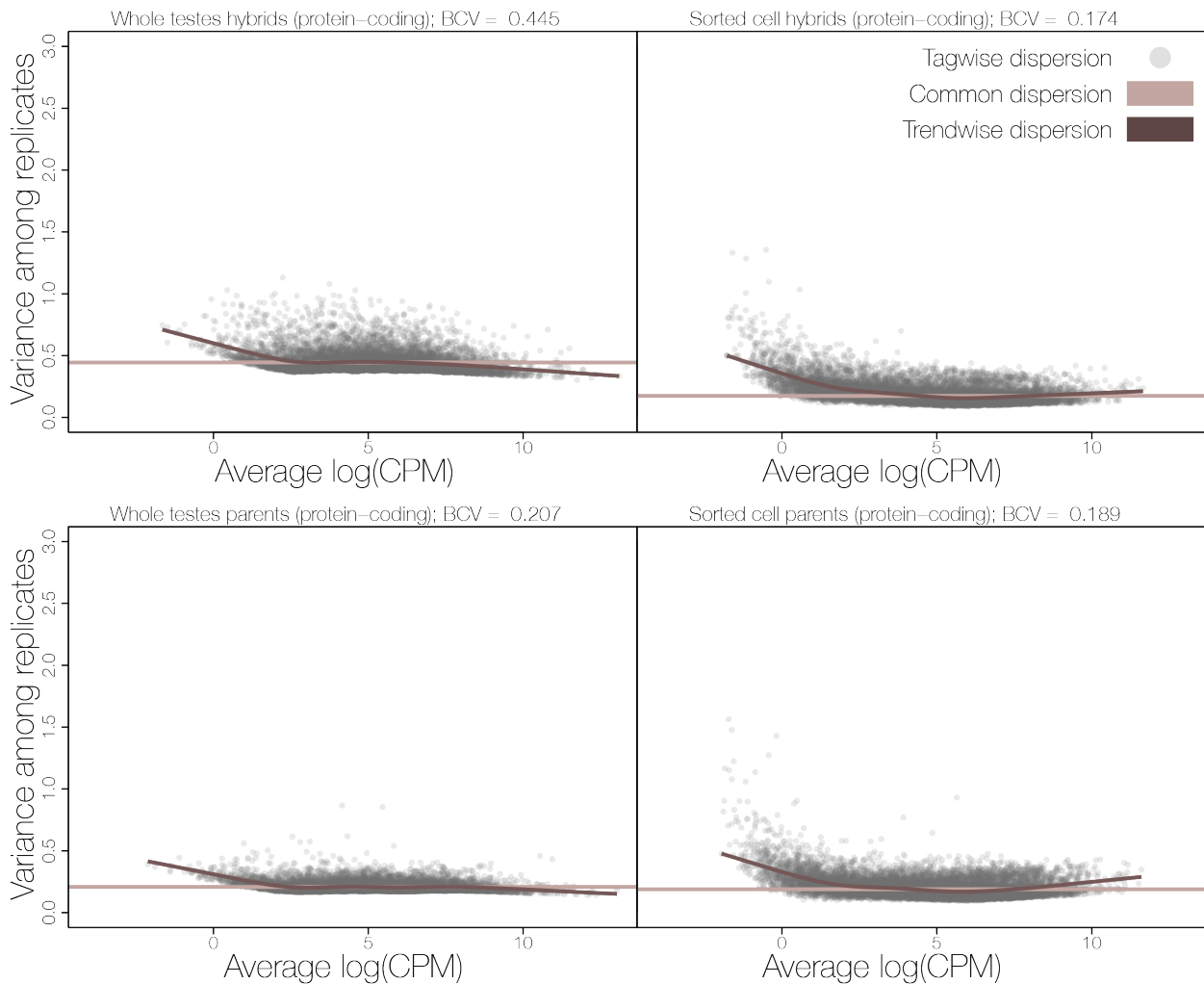


Fig S3. Dispersion estimates and biological coefficient of variation (BCV) calculations across protein-coding genes for parental and hybrid samples separately for the whole testes and sorted cell datasets. All dispersion estimates were calculated in R with the edgeR package (McCarthy et al. 2012). Common dispersion for each dataset is calculated using a common estimate across all genes (taupe line). The trendwise dispersion calculation fits an estimate of dispersion based on the mean-variance trend across the entire dataset so that genes with similar abundances have similar variance estimates (brown line). Tagwise dispersion estimates dispersion on a per gene basis (gray dots). The BCV is the square root of the common dispersion.

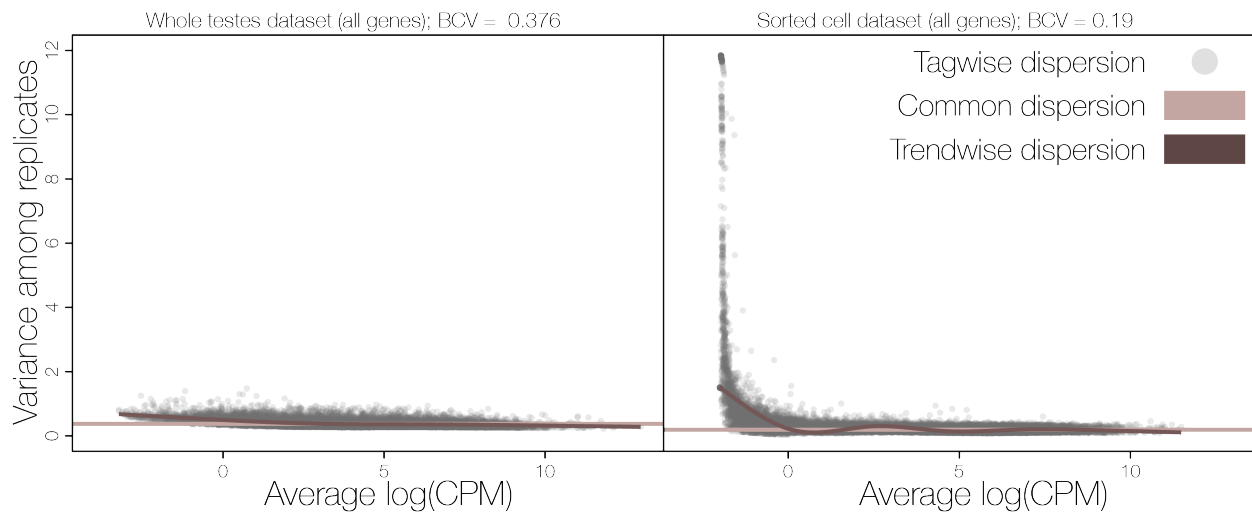


Fig S4. Dispersion estimates and biological coefficients of variation (BCV) across all genes for the whole testes and sorted cell datasets. All dispersion estimates were calculated in R with the edgeR package (McCarthy et al. 2012). Common dispersion for each dataset is calculated using a common estimate across all genes (taupe line). The trendwise dispersion calculation fits an estimate of dispersion based on the mean-variance trend across the entire dataset so that genes with similar abundances have similar variance estimates (brown line). Tagwise dispersion estimates dispersion on a per gene basis (gray dots). The BCV is the square root of the common dispersion.

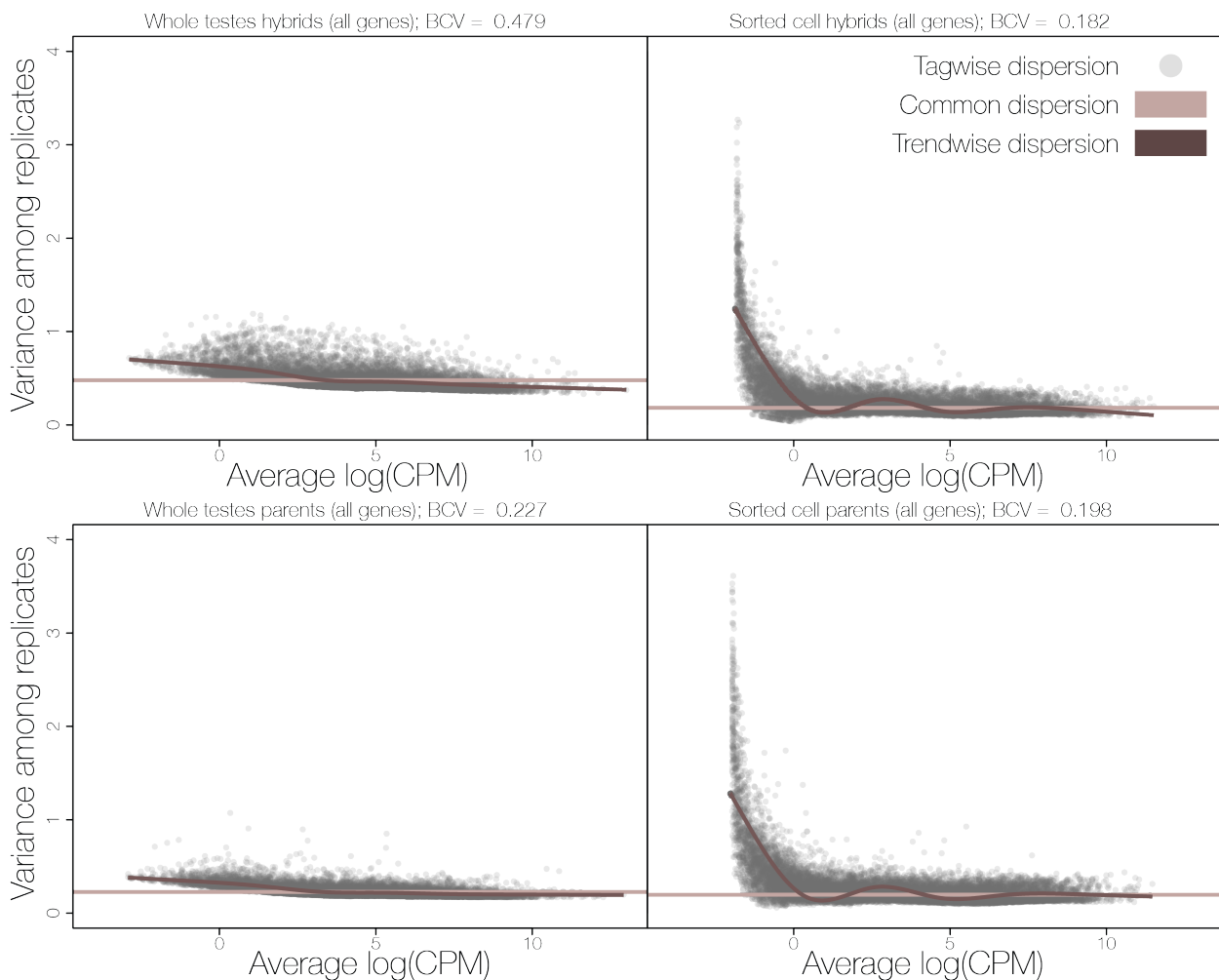


Fig S5. Dispersion estimates and biological coefficient of variation (BCV) calculations across all genes for parental and hybrid samples separately for the whole testes and sorted cell datasets. All dispersion estimates were calculated in R with the edgeR package (McCarthy et al. 2012). Common dispersion for each dataset is calculated using a common estimate across all genes (taupe line). The trendwise dispersion calculation fits an estimate of dispersion based on the mean-variance trend across the entire dataset so that genes with similar abundances have similar variance estimates (brown line). Tagwise dispersion estimates dispersion on a per gene basis (gray dots). The BCV is the square root of the common dispersion.

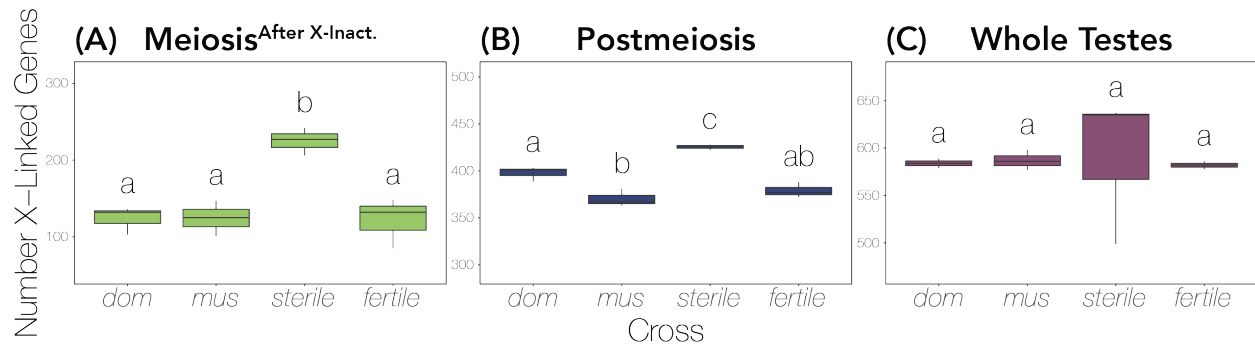


Fig S6. Overexpression of the X chromosome in sterile hybrids is detectable in sorted cell populations but not whole testes. Mean number of X-linked genes for each cross within a sample type with a minimum expression of one FPKM across all samples within a dataset (sorted cells or whole testes). Whiskers show 95% confidence intervals. Different letters above error bars indicate a significant difference between means at $p<0.05$ using a post-hoc Tukey HSD test. Each panel shows results from three sample types, Meiosis^{After X-Inact.} (**A**; green), Postmeiosis (**B**; blue), and Whole Testes (**C**; purple).

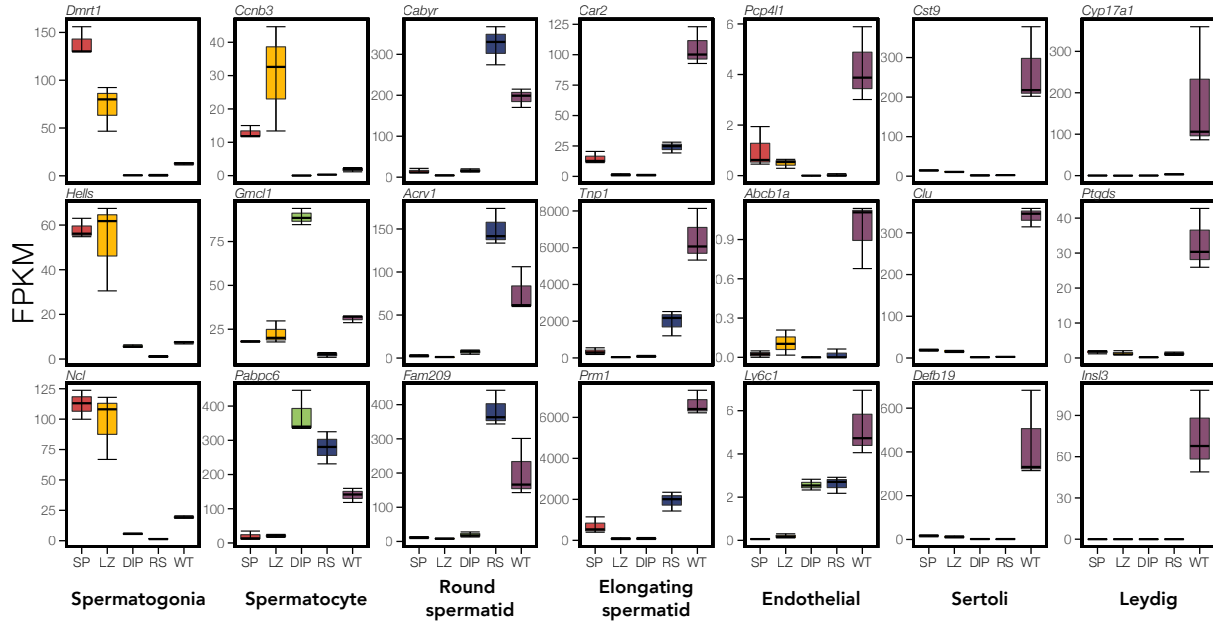


Fig S7. Whole testes expression profiles show signatures of many diverse cell types.

Expression of cell-specific marker genes across each sample type for *mus* reference samples. We quantified expression (FPKM) of three marker genes (rows) associated with testes-specific cell types (columns). Each panel displays marker expression in each sample type (red = Mitosis (SP), yellow = Meiosis^{Before X-Inact.} (LZ), green = Meiosis^{After X-Inact.} (DIP), blue = Postmeiosis (RS), and purple = Whole Testes (WT)). Note, *Ccnb3* expression is specific to Meiotic^{Before X-Inact.} cells (Maekawa et al. 2004), and *Gmc1* is specific to Meiotic^{After X-Inact.} cells (Nguyen et al. 2002).

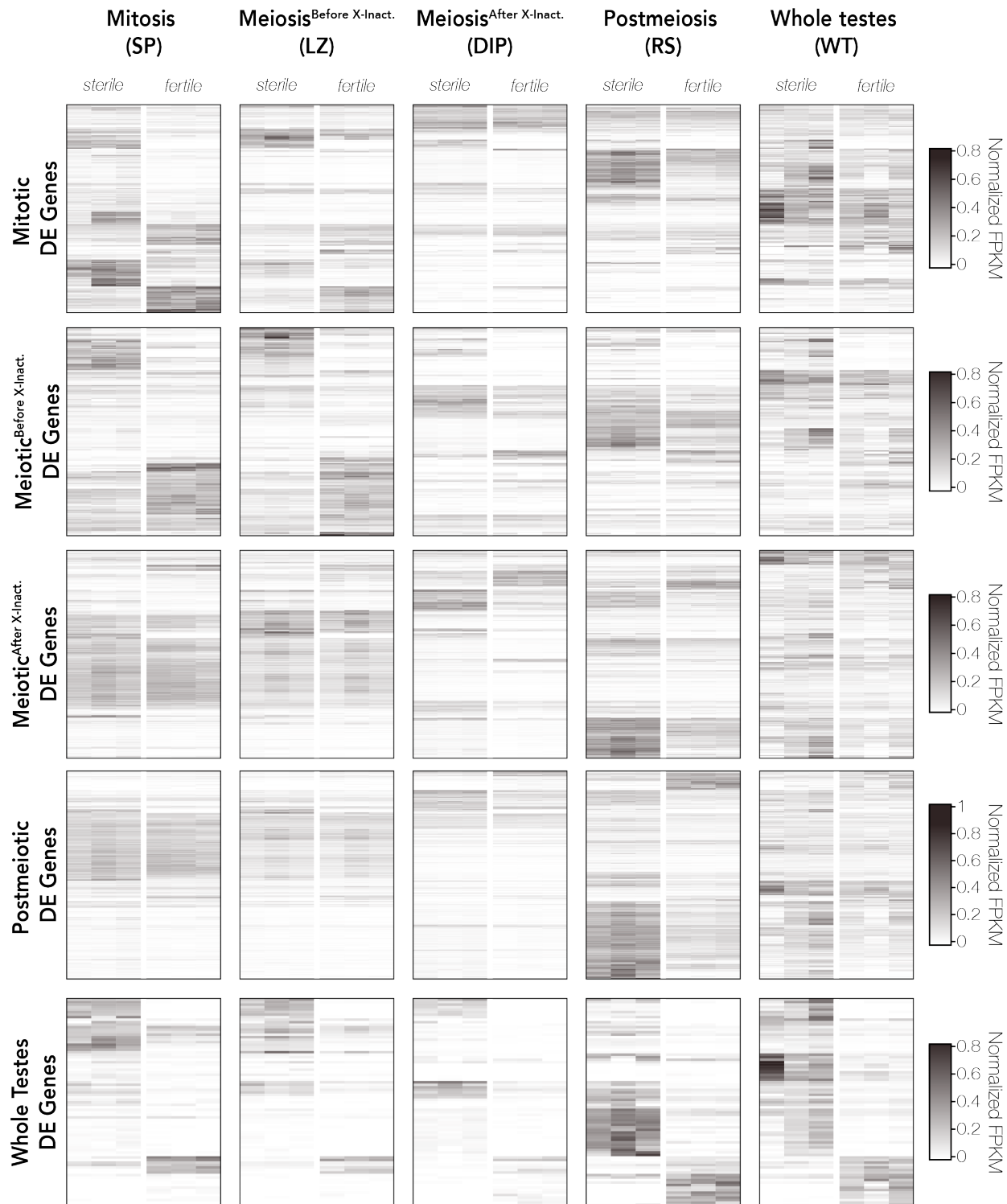


Fig S8. Expression of sample-type specific DE genes in sterile and fertile hybrids across all sample types. FPKM values were normalized so that the sum of squares equals one using the R package vegan (Oksanen et al. 2007). Beanplots were generated with the R package beanplot (Kampstra 2008). Each heatmap has gene expression plotted as normalized FPKM values that

are hierarchically clustered using Euclidean distance. Each row plots expression across one gene and darker colors indicate higher expression. Heatmaps were generated with the R package ComplexHeatmap v.2.3.2 (Gu et al. 2016).

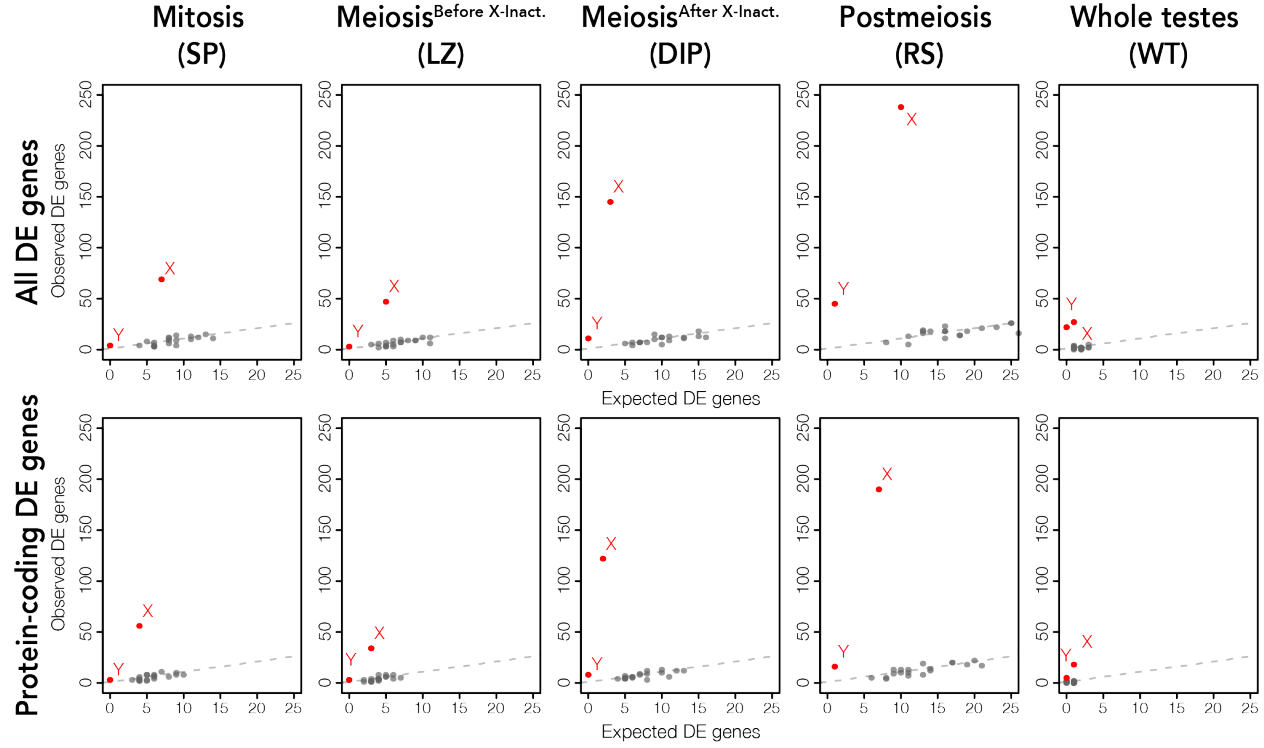


Fig S9. Sex chromosomes are enriched for DE genes across all stages. For each sample type, a scatter plot displays expected versus observed counts of DE genes for each chromosome. Chromosomes above the dashed line are over-enriched for DE genes, and chromosomes below the dashed line are under-enriched for DE genes, with chromosomes where p-values were less than 0.001 after FDR correction are highlighted in red and labelled. Upper panels are DE genes from all annotated genes and lower panels are DE genes from only protein-coding genes.

Supplemental Tables:

Table S1: Sample information and read counts. Sample IDs correspond to the cross of the individual (CC = CZECHII/EiJ, LL = LEWES/EiJ, PP = PWK/PhJ, and WW = WSB/EiJ), the individuals ID number, and the sample type (SP = Mitosis, LZ = Meiosis^{Before X-Inact.}, DIP = Meiosis^{After X-Inact.}, RS = Postmeiosis, and WT = Whole Testes).

Sample ID	SRA Accession	Raw Reads (F only)	Post-Tophat PWK-Alignment Reads (F+R)	Post-Tophat WSB-Alignment Reads (F+R)	Post-Suspenders Reads (F+R)	Assigned FeatureCount Read Pairs (no multi-mapped reads)
CCPP-21.1-DIP	SRR2761570, SRR2761592	21477056	26340755	25674973	19232543	7381118
CCPP-21.1-LZ	SRR2761571, SRR2761593	26998246	33134843	32416769	23610512	8867722
CCPP-21.1-RS	SRR2761572, SRR2761594	22195796	35312787	34717874	19809616	7721308
CCPP-21.1-SP	SRR2761573, SRR2761595	31751428	38868844	37967473	27275613	9931488
CCPP-21.2-DIP	SRR2761596	36852964	46965915	45728821	33544699	12803354
CCPP-21.2-LZ	SRR2761574, SRR2761597	26549896	32060131	31287872	23526641	8786313
CCPP-21.2-RS	SRR2761598	22235268	36029725	35270117	20281803	7942450
CCPP-21.2-SP	SRR2761575, SRR2761599	28802542	34567190	33765425	24615826	8998231
CCPP-21.3-DIP	SRR2761549, SRR2761600	22468784	27090066	26309504	20152293	7764490
CCPP-21.3-LZ	SRR2761550, SRR2761601	20428992	24566552	23933367	17891667	6709337
CCPP-21.3-RS	SRR2761602	32112934	45597240	44284041	28554464	11260227
CCPP-21.3-SP	SRR2761551, SRR2761603	21751826	26924883	26217413	19057748	7075581
LLPP-17.2-DIP	SRR2761576, SRR2761604	19989428	24880530	24872825	18021849	6822392
LLPP-17.2-RS	SRR2761577, SRR2761605	22525160	33916646	33841987	20044435	7762604
LLPP-18.1-LZ	SRR2761578, SRR2761606	27817084	35876214	35985195	24854243	8985489
LLPP-19.1-DIP	SRR2761552, SRR2761607	18058676	22479413	22438712	16204722	6096994
LLPP-19.1-SP	SRR2761579, SRR2761608	33430222	39885520	39708715	28440056	10028665
LLPP-19.2-RS	SRR2761553, SRR2761609	18407584	28601605	28594856	16484648	6323895
LLPP-19.3-DIP	SRR2761554, SRR2761610	19415690	23093669	23054030	17375360	6661074
LLPP-19.3-RS	SRR2761555, SRR2761611	19781658	27402180	27494017	17681421	6959808
LLPP-22.7-LZ	SRR2761556, SRR2761612	20036778	25245447	25262290	17820330	6477961
LLPP-22.7-SP	SRR2761557, SRR2761613	18338020	22593735	22567117	16094821	5971162
LLPP-22.8-LZ	SRR2761558, SRR2761614	23411888	29264006	29336299	21033663	7685705
LLPP-22.8-SP	SRR2761559, SRR2761615	19297400	22586043	22519133	16561826	6017707
LLPP-272-WT	SRR2060953	124219124	142525063	142380020	108427854	42898717
LLPP-290-WT	SRR2060952	34464432	38526459	38543523	32163922	13313386
LLPP-93-WT	SRR2060950	63070002	47005603	47097532	34088411	12586942
LLWW-148-WT	SRR2060837	101248844	74722027	77167079	54406591	19891163
LLWW-149-WT	SRR2060842	107432468	128083415	130793609	93850300	35897894
LLWW-150-WT	SRR2060843	100497198	108902509	111315069	81179922	31309028

PPCC-151-WT	SRR2060844	76325172	58327482	56337894	39979615	14783396
PPCC-152-WT	SRR2060846	98804204	118179509	115163595	85840471	33494033
PPCC-170-WT	SRR2060939	76594232	90758054	88360116	66410204	25980058
PPLL-131-WT	SRR2060954	24882156	28222294	28244608	23110713	9474627
PPLL-15.2-DIP	SRR2761580, SRR2761616	23647380	30142023	29984831	21268666	8069338
PPLL-15.2-RS	SRR2761581, SRR2761617	23128976	40531135	40317066	20658116	7842258
PPLL-16.1-DIP	SRR2761560, SRR2761618	20048656	24991779	24867469	17763716	6646884
PPLL-16.1-LZ	SRR2761561, SRR2761619	21281980	27273010	27117068	18786051	6912012
PPLL-16.1-RS	SRR2761562, SRR2761620	19168394	29754797	29751712	16517064	6361843
PPLL-16.1-SP	SRR2761563, SRR2761621	22451632	27796017	27662178	19388612	7051214
PPLL-17.1-DIP	SRR2761622	37268646	45864903	45637800	33049299	12492601
PPLL-17.1-LZ	SRR2761582, SRR2761623	30492632	41043284	40790863	27195859	9923511
PPLL-17.1-RS	SRR2761624	25277730	40651852	40533661	22361132	8609292
PPLL-17.1-SP	SRR2761583, SRR2761625	33687062	40791246	40560457	29439375	11005974
PPLL-17.3-LZ	SRR2761564, SRR2761626	19742116	25086723	24944022	17398240	6412712
PPLL-17.3-SP	SRR2761565, SRR2761627	23598202	28711605	28465007	20271530	7299012
PPLL-278-WT	SRR2060955	102188034	133331212	133813859	89775343	33934908
PPLL-52-WT	SRR2060951	44950474	53997983	53670612	35822322	12838352
WWLL-3.1-DIP	SRR2761584, SRR2761628	21970318	26565246	27212060	19982585	7588358
WWLL-3.1-RS	SRR2761585, SRR2761629	22523002	33735184	34378293	20360830	7972083
WWLL-3.1-SP	SRR2761566, SRR2761630	21104146	25684138	26185875	18283388	6458669
WWLL-4.1-LZ	SRR2761567, SRR2761631	20075246	25176105	25778595	17983406	6642792
WWLL-6.1-RS	SRR2761568, SRR2761632	20388762	29125360	29720516	18060410	7053241
WWLL-7.1-DIP	SRR2761569, SRR2761633	19974584	23300740	24024169	17794108	6798887
WWLL-7.2-DIP	SRR2761586, SRR2761634	20182808	24558522	25232730	18511737	6969049
WWLL-7.2-LZ	SRR2761587, SRR2761635	20087232	25629600	26319298	18253476	6675109
WWLL-7.2-RS	SRR2761588, SRR2761636	20822386	28662881	29206953	18976974	7607417
WWLL-7.2-SP	SRR2761589, SRR2761637	25852196	32343831	33080949	22904315	8266300
WWLL-7.3-LZ	SRR2761590, SRR2761638	41266036	53274705	54449278	37203850	13432758
WWLL-7.3-SP	SRR2761591, SRR2761639	35512824	43398931	44340114	31279482	11230973

Table S2: Counts of different categories of hybrid DE genes for each sample type.

Stage	X-linked DE genes	Y-linked DE genes	Autosomal DE genes	Up-regulated in sterile	Down-regulated in sterile	Total DE genes
Mitosis	69	4	158	152	79	231
Meiosis ^{Before X-Inact.}	47	3	128	88	90	178
Meiosis ^{Before X-Inact.}	145	11	187	284	59	343
Postmeiosis	238	45	323	497	109	606
Whole Testes	27	22	34	63	20	83

Table S3: Direction of regulation (relative to *sterile*) for hybrid DE genes in whole testes and each sorted cell populations for each pairwise comparison.

Comparison	Up in WT & down in sorted cell population	Down in WT & up in sorted cell population	Up-regulated in both	Down-regulated in both	Misregulated between sorted cell population and whole testes (%)
Mitosis and WT	0	0	25	6	0
Meiosis ^{Before X-Inact.} and WT	0	0	22	5	0
Meiosis ^{Before X-Inact.} and WT	0	0	28	5	0
Postmeiosis and WT	0	0	47	17	0

Table S4: Direction of regulation (relative to *mus*) for DE genes between *dom* and *mus* in whole testes and each sorted cell populations for each pairwise comparison.

Comparison	Up in WT & down in sorted cell population	Down in WT & up in sorted cell population	Up-regulated in both	Down-regulated in both	Misregulated between sorted cell population and whole testes (%)
Mitosis and WT	22	14	392	712	3.26
Meiosis ^{Before X-Inact.} and WT	10	15	357	553	2.75
Meiosis ^{Before X-Inact.} and WT	11	14	557	757	1.9
Postmeiosis and WT	5	3	721	1130	0.43

LITERATURE CITED

- Gu, Z., R. Eils, and M. Schlesner. 2016. Complex heatmaps reveal patterns and correlations in multidimensional genomic data. *Bioinformatics* 32:2847–2849.
- Kampstra, P. 2008. Beanplot: A boxplot alternative for visual comparison of distributions. *J. Stat. Softw.* 28.
- Maekawa, M., C. Ito, Y. Toyama, F. Suzuki-Toyota, T. Kimura, T. Nakano, and K. Toshimori. 2004. Stage-specific expression of mouse germ cell-less-1 (mGCL-1), and multiple deformations during mgcl-1 deficient spermatogenesis leading to reduced fertility. *Arch. Histol. Cytol.* 67:335–347.
- McCarthy, D. J., Y. Chen, and G. K. Smyth. 2012. Differential expression analysis of multifactor RNA-Seq experiments with respect to biological variation. *Nucleic Acids Res.* 40:4288–4297.
- Nguyen, T. B., K. Manova, P. Capodieci, C. Lindon, S. Bottega, X.-Y. Wang, J. Refik-Rogers, J. Pines, D. J. Wolgemuth, and A. Koff. 2002. Characterization and expression of mammalian cyclin b3, a prepachytene meiotic cyclin. *J. Biol. Chem.* 277:41960–41969.
- Oksanen, J., R. Kindt, P. Legendre, B. O’Hara, M. H. H. Stevens, M. J. Oksanen, and M. Suggs. 2007. The vegan package. *Community ecology package* 10:719.